

RESEARCH

Open Access



The acyltransferase transmembrane protein 68 regulates breast cancer cell proliferation by modulating triacylglycerol metabolism

Zheng Zhao¹, Huimin Pang¹, Qing Yu¹, Fansi Zeng¹, Xiaohong He¹, Quan Sun¹ and Pingan Chang^{1*}

Abstract

Background Cellular carcinogenesis is often marked by the accumulation of lipid droplets (LDs) due to reprogrammed lipid metabolism. LDs are dynamic organelles that primarily store intracellular triacylglycerol (TAG) and cholesteryl esters (CEs). Transmembrane protein 68 (TMEM68), a potential modifier of human breast cancer risk and outcomes, functions as a diacylglycerol acyltransferase, synthesizing TAG. However, the specific roles of TMEM68 in breast cancer cells remain unclear.

Methods Gene expression profiling interactive analysis and survival analysis were conducted. TMEM68 was overexpressed or knockdown in breast cancer cells to assess its impact on cell proliferation, migration and invasion. Targeted quantitative lipidomic analysis and quantitative polymerase chain reaction were used to profile lipid alterations and examine gene expression related to lipid metabolism following changes in TMEM68 levels.

Results *TMEM68* gene was upregulated in breast cancer patients and higher TMEM68 levels were associated with poorer survival outcomes. Overexpression of TMEM68 increased breast cancer cell proliferation and invasion, whereas knockdown had minimal or no impact on reducing proliferation and invasion. Altering TMEM68 levels resulted in corresponding changes in TAG levels and cytoplasmic LDs, with overexpression increasing both and knockdown decreasing them. Lipidomic analysis revealed that TMEM68 regulated TAG levels and altered diacylglycerol content in breast cancer cells. Additionally, TMEM68 influenced the metabolism of glycerophospholipids, CEs and acylcarnitines. TMEM68 also modified the expression of key genes encoding enzymes related to neutral lipid metabolism, including TAG and CEs.

Conclusions TMEM68 is highly expressed in breast cancer and negatively correlated with survival. Its overexpression promotes breast cancer cell proliferation while knockdown has varied effects depending on TMEM68 levels. TMEM68 regulates intracellular TAG and LDs contents along with alterations in glycerophospholipids. These findings suggest that TMEM68 may drive breast cancer cells proliferation by modulating TAG and LD content.

Keywords Triacylglycerol, Lipid droplet, Breast cancer cell proliferation, Glycerophospholipid, Transmembrane protein 68

*Correspondence:

Pingan Chang
changpa@cqupt.edu.cn

¹Chongqing Key Laboratory of Big Data for Bio-Intelligence, School of Life Health Information Science and Engineering, Chongqing University of Posts and Telecommunications, Chongqing 400065, China



© The Author(s) 2024. **Open Access** This article is licensed under a Creative Commons Attribution-NonCommercial-NoDerivatives 4.0 International License, which permits any non-commercial use, sharing, distribution and reproduction in any medium or format, as long as you give appropriate credit to the original author(s) and the source, provide a link to the Creative Commons licence, and indicate if you modified the licensed material. You do not have permission under this licence to share adapted material derived from this article or parts of it. The images or other third party material in this article are included in the article's Creative Commons licence, unless indicated otherwise in a credit line to the material. If material is not included in the article's Creative Commons licence and your intended use is not permitted by statutory regulation or exceeds the permitted use, you will need to obtain permission directly from the copyright holder. To view a copy of this licence, visit <http://creativecommons.org/licenses/by-nc-nd/4.0/>.

Introduction

The incidence and associated mortality rates of breast cancer, as the most frequent cancer among women are steadily rising worldwide [1, 2]. Based on gene expression, highly complex and heterogeneous breast cancer is usually classified into four distinct subtypes [3–5]. Luminal A tumors are positive for estrogen receptor (ER) and progesterone receptor (PR), but negative for CK5/6, epidermal growth factor receptor (EGFR) and human epidermal growth factor receptor 2 (HER2). Luminal B tumor have lower expression of ER and PR and exhibit high histologic grade. HER2-positive tumors subtype may be HER2 positive, but negative for CK5/6, EGFR, ER, and PR. Triple-negative breast cancer (TNBC) lacks ER and PR expression and shows no amplification of the *HER2* gene [3–5].

Metabolic reprogramming, an established hallmark of cancer, has been identified as a prerequisite for cancer initiation and progression [6]. Lipids provide energy, form the backbone for membrane synthesis, and act as mediators of signal transduction in cancer cells. Regulating lipid metabolism is considered an effective strategy for cancer cells adapt to changing microenvironments and has attracted extensive research attention in recent years [7]. LDs accumulation is a common feature of cellular carcinogenesis and often accompanies lipid metabolism reprogramming [8]. In breast cancer cells, LD expansion enhances cell survival during hypoxia and protects cells against nutrient and oxidative stress [9–12]. High LD content is also associated with breast cancer cell stemness as well as drug and radiation therapy resistance [13–15].

Neutral lipids, primarily TAG and CE are stored in the hydrophobic core of LD [16]. With the exception of the monoacylglycerol (MAG) pathway that is largely restricted to enterocytes, the glycerol-3-phosphate (G3P) pathway is primarily responsible for the *de novo* synthesis of TAG in most mammalian cells (Supplementary Fig. S1) [17, 18]. Both pathways share a common final reaction, incorporating a fatty acid from acyl-CoA into diacylglycerol (DAG), which is catalyzed by the acyl-CoA: diacylglycerol acyltransferases (DGATs), DGAT1 and DGAT2, the key enzymes in TAG synthesis [17, 18]. In contrast, TAG is initially mobilized by adipose triglyceride lipase (ATGL), the rate-limiting enzyme during lipolysis [19]. All of them are implicated in breast cancer progression [8, 20]. Additionally, enzymes participated in fatty acid synthesis contribute to breast cancer tumorigenesis [21, 22].

The putative acyltransferase transmembrane protein 68 (TMEM68) forms a distinct subgroup in the pfam01553 glycerophospholipid acyltransferase family [23], although its role in TAG metabolism in breast cancer remain unclear. Several enzymes in the G3P pathway, including

glycerophosphate acyltransferase (GPAT) and acylglycerophosphate acyltransferase (AGPAT) also belong to this family [23]. Akin to GPAT/AGPAT, TMEM68 contains the most conserved motif I in the pfam01553 domain with the conserved active sites H and D forming an acyltransferase catalytic dyad [23, 24]. TMEM68 has two putative transmembrane domains and is localized to the endoplasmic reticulum via the first transmembrane domain [24]. Overexpression of TMEM68 elevated TAG levels and enhanced LD accumulation in HEK293 and MCF-7 cells, depending on the conserved catalytic motif I [25]. An *in vitro* assay revealed that TMEM68 exhibited monoacylglycerol acyltransferase (MGAT) and DGAT activity [25]. TMEM68 mediates an alternative pathway for TAG synthesis independent of DGAT and possibly incorporate fatty acyl groups from phospholipids into DAG to form TAG (Fig. S1) [26]. TMEM68 activity is blocked by the endoplasmic reticulum-anchored transmembrane thioredoxin 1 (TMX1), and deletion of TMX1 triggers TMEM68 activity, resulting in higher than basal levels of TAG in cells [26]. *Tmem68* knockout in mice led to around a 50% reduction in fat mass and lowered TAG levels in serum and brain tissue [26]. Thus, TMEM68 plays a critical role in TAG biosynthesis.

Expression levels of the rat *TMEM68* gene are higher in susceptible breast tumors than in resistant mammary tumors, suggesting that TMEM68 may be a potential modifier of breast cancer risk and outcomes in humans [27]. Given its role in TAG biosynthesis, TMEM68 likely influences breast cancer cells by regulating lipid metabolism, particularly TAG homeostasis. Given the complex effects of lipids on tumor development, it is essential to analyze biological samples using methods that can assess multiple lipid species rather than focusing on a single lipid class. In the current study, TMEM68 was demonstrated to regulate the proliferation of breast cancer cells, and modulate global lipid homeostasis, especially levels of TAG and glycerophospholipids (GPLs).

Materials and methods

Gene expression profiling and survival analysis

Gene expression, overall survival (OS) and disease-free survival (DFS) analyses of TMEM68 in breast cancer patients were conducted on Gene Expression Profiling Interactive Analysis (GEPIA) website (<http://gepia.cancer-pku.cn/>) [28]. In total, 1085 breast invasive carcinoma (BRCA) samples and 291 normal breast tissue samples were included. Box plots and stage plots for the *TMEM68* gene were generated to analyze gene expression profiles in BRCA and paired normal samples. Survival differences for disease-free interval (DFI) and metastasis-free survival (MFS) were analyzed between high- and low-TMEM68 levels groups using the R package “survival”. *P*-values were determined using Log-rank

tests. TMEM68 protein expression detected by immunohistochemistry (IHC) was from The Human Protein Atlas (<https://www.proteinatlas.org>).

Cell culture and treatment

SK-BR-3 cells were cultured in Dulbecco's modified Eagle medium (DMEM) supplemented with 10% fetal bovine serum (FBS), 100 units/mL penicillin and 100 µg/mL streptomycin. MCF-7 cells were cultured in DMEM containing FBS, penicillin, streptomycin, and 10 µg/mL insulin. BT-474 cells were cultured in RPMI 1640 supplemented with 20% FBS, penicillin and streptomycin, 10 µg/mL insulin and 200 µg/mL L-glutamine. SK-BR-3, MCF-7 and BT-474 cells were maintained at 37 °C in saturated humidity with 5% CO₂. MDA-MB-453 cells were cultured in L-15 medium supplemented with 10% FBS,

penicillin and streptomycin, 10 µg/mL insulin, in a 37 °C incubator with saturated humidity. 0.2 mM oleic acid (OA) complexed with fat-free bovine serum albumin was loaded into medium for 12 h to induce TAG biosynthesis.

Generation of lentivirus and stable infection

To stably express and knockdown human TMEM68, lentiviral particles were generated and then transduced into MCF-7 cells as previous description [29]. Briefly, lentiviral particles containing vectors expressing the human TMEM68 protein were produced by VectorBuilder (Guangzhou, China). Lentiviral plasmids encoding scrambled shRNA or shRNA targeting human TMEM68 (shTMEM68: 5'-TTCCTGGATAATGCGTTAAATCTCGAGATTTAACGCATTATCCAGGAA-3') were constructed and lentiviral particles were generated by Cyagen Biosciences (Suzhou, China). Cells (3×10⁵ per well) were seeded into 6-well plates and transduced with lentiviral particle and polybrene (8 µg/mL) for 24 h the next day. Stable expressing cell clones were then selected with puromycin (2 µg/mL) for one week. Positive clones for overexpression or knockdown were verified by quantitative polymerase chain reaction (qPCR).

Table 1 The primers used for qPCR

Primer name	Sequence (5'-3')
TMEM68F	CGGGTGCAGAAAACCTCCAG
TMEM68R	CGCATAATCTTCCGGCCATAGA
ATGLF	GAGATGTGCAAGCAGGGATAC
ATGLR	CTGCGAGTAATCTCCCGCT
HSLF	GACCCCTGCACAACATGATG
HSLR	TGAGCAGCACCCCTTTGGATG
DGAT1F	GGTCCCCAATCACCTCATCTG
DGAT1R	TGCACAGGGATGTTCCAGTTC
DGAT2F	ATTGCTGGCTCATCGCTGT
DGAT2R	GGGAAAGTAGTCTCGAAAGTAGC
FASNF	AAGGACCTGTCTAGGTTTGATGC
FASNR	TGGCTTCATAGGTGACTTCCA
SCD1F	TTCCTACCTGCAAGTTCTACACC
SCD1R	CCGAGCTTTGTAAGAGCGGT
ACACAF	TCACACCTGAAGACCTTAAAGCC
ACACAR	AGCCCACTGCTTGTACTG
SOAT1F	GGTGCCTCTCACAACTTT
SOAT1R	GAGGTGCTCTCAAATCCTTCG
SOAT2F	ATGAAACACTGAGACGCACA
SOAT2R	GGTAGGATTATATAGCCTCCCG
PPARαF	TTCGCAATCCATCGGCGAG
PPARαR	CCACAGGATAAGTCACCGAGG
PPARγF	TACTGTCGGTTTCAGAAATGCC
PPARγR	GTCAGCGGACTCTGGATTACAG
actinF	CATGTACGTTGCTATCCAGGC
actinR	CTCCTTAATGTCACGCACGAT
GPAT1F	GATGTAAGCACACAAGTGAGGA
GPAT1R	TCCGACTCATTAGGCTTTCTTTC
GPAT2F	TGTGGTCGTCAGGCTTTGG
GPAT2R	GGTCCGTTATGCTTCTGTGGA
GPAT3F	CGCTGGTTCTCGGCTTCAT
GPAT3R	TGGCCCACTCTAAAGTTTTAC
GPAT4F	GGTATCCGCAAACCTCATATGAA
GPAT4R	CCACTTCGACGAATCTCTTTGA
TMX1F	TTGCGAAAGTAGATGTCACAGAG
TMX1R	CTGATAGCGCCTAAATCACCAT

RNA extraction and qPCR

Total RNA was prepared using the Total RNA Isolation Kit V2 (Vazyme Biotechnology, Nanjing, China) according to the manufacturer's instructions. Reverse transcription (RT)-qPCR was carried out using RT mixture with a DNase (Yuhon Biotechnologies, Suzhou, China) and SYBR Mix (Vazyme Biotechnology) on a Bio-Rad IQ5 qPCR system. Gene expression were determined based on the $\Delta\Delta C_t$ method using β -actin as reference gene [30]. Primers were listed in Table 1.

Immunoblotting analysis

Total protein was prepared by sonication in RIPA buffer containing 1 mM phenylmethylsulfonyl fluoride (PMSF) and then centrifuged at 15,000 g and 4 °C for 10 min to precipitate cellular debris. Protein concentration was measured using a BCA protein assay kit (Beyotime Biotechnology, Shanghai, China). The supernatant samples were mixed with Laemmli buffer, denatured at 98 °C for 5 min, subjected to SDS-PAGE, and electroblotted onto nitrocellulose membranes. Membranes were incubated in TBST buffer containing 5% milk for 1 h to block nonspecific binding. TMEM68 expression was detected by immunoblotting with an anti-TMEM68 antibody (Abmart Biotechnology, Shanghai, China; 1:1000 diluted in TBST containing 5% milk), as described previously [31]. GAPDH protein levels were used as a loading control.

Cell proliferation assay

Cell viability was assessed using a Cell Counting Kit-8 (CCK-8; Solarbio Life Sciences, Beijing, China) at 24, 48, 72, and 96 h post seeding. Cells were seeded in 96-well plates at a density of 5×10^3 cells/well. After removing medium at the indicated times, cells were incubated with complete medium supplemented with 10% well-mixed CCK-8 reagent for 2 h. Absorbance at 450 nm was then measured using a microplate reader (Detie, Nanjing, China).

Cell migration and invasion assays

The cells were plated in triplicates in the upper wells of 24-well transwell chambers (8.0 μ m pore size) at a density of 1×10^5 per well in 100 μ L of serum-free medium. At the same time, 600 μ L of complete medium containing 20% FBS was added to the lower chamber. After a period of 48 h migration at 37 °C and 5% CO₂ atmosphere, cells remaining at upper membrane surface of the upper wells were removed by wiping with a cotton swab. Cells that migrated to the lower surface of filter were fixed with 4% paraformaldehyde for 20 min and stained with 0.5% crystal violet solution for 15 min.

The transwell invasion assay was performed as described above, except that 100 μ L of 1:8 serum-free medium-diluted Matrigel (Corning, Shanghai, China) was added to each well at 37 °C for 2 h before the cells were seeded onto the membrane, followed by a 48-h incubation. The cells that passed through the filter were photographed using an inverted microscope. The cell migration and invasion were scored by counting five random fields per filter under a light microscope.

Oil red O staining

Cells were washed briefly twice after removing medium with phosphate-buffered saline (PBS), and then fixed with 4% paraformaldehyde at room temperature for 15 min. Neutral lipids were stained using an Oil Red O kit (Solarbio Life Sciences). Images were then captured using an inverted microscope.

TAG level measurement

TAG levels were determined using the Triglyceride Assay Kit E1025 (Applygen, Beijing, China), as previously described [25]. Briefly, cells were harvested and dissolved in lysis buffer. Cell lysates were briefly centrifuged, and supernatants was heated at 70 °C for 10 min and further centrifuged at 2000 rpm for 5 min. TAG levels in the supernatants were measured following the manufacturer's protocol.

Confocal fluorescence microscopy

Cells were cultured in 12-well plates and mounted onto coverslips. The following day, cells were fixed with 4%

paraformaldehyde at room temperature for 30 min and then washed briefly with PBS. LDs were stained with HCS LipidTOX™ Deep Red (ThermoFisher Scientific, Waltham, MA, USA; 1:1000 dilution in PBS) for 30 min. Nuclei were stained with 0.5 μ g/mL 4',6-diamidino-2-phenylindole (DAPI) for 15 min. Slides were sealed with antifade mounting medium and cells were imaged using an Olympus SpinSR confocal microscope. HCS LipidTOX™ Deep Red was excited at 633 nm, and emission was detected at 650–700 nm. DAPI was excited at 364 nm, and emission was detected at 450–490 nm.

Quantitative lipidomic analysis

Lipid extraction and targeted lipidomic analyses were performed by LipidALL Technologies (Changzhou, China). Approximately 1×10^7 cells were used to extract lipids with a modified Bligh and Dyer's method as described previously [32]. Briefly, cells were homogenized in a 750 μ L solution containing chloroform: methanol: Milli-Q H₂O (volume ratio: 3:6:1), and then incubated at 1500 rpm and 4 °C for 1 h. Adding 250 μ L of chloroform and 350 μ L of deionized water to induce phase separation. Lipid extraction was repeated once by adding 450 μ L of chloroform to the remaining cells in aqueous phase, and the lipid extracts were pooled into a single tube and dried in the SpeedVac under OH mode. Upper aqueous phase and cell pellet were dried in a SpeedVac under H₂O mode. Total protein content was determined from the dried pellet using the Pierce® BCA Protein Assay Kit according to the manufacturer's protocol. Samples were stored at -80 °C until further analysis.

Lipidomic analyses were conducted at LipidALL Technologies using a Jasper high-performance liquid chromatography (HPLC) system coupled with Sciex TRIPLE QUAD 4500 MD as reported previously [33]. Separation of individual lipid classes by normal phase (NP)-HPLC was carried out using a TUP-HB silica column (i.d. 150 \times 2.1 mm, 3 μ m) with the following conditions: mobile phase A (chloroform: methanol: ammonium hydroxide, 89.5:10:0.5) and mobile phase B (chloroform: methanol: ammonium hydroxide: water, 55:39:0.5:5.5). Multiple reaction monitoring (MRM) transitions were set up for comparative analysis of various lipids (Supplementary Table 1). Individual lipid species were quantified by referencing to spiked internal standards. d9-PC32:0(16:0/16:0), PE 34:0, dic8-PI, d31-PS, C17:0-PA, DMPG, CL-14:0, C14-BMP, C12-SL, C17-LPC, C17-LPE, C17:1-LPI, C17:0-LPA, C17:1-LPS, C17-Cer, C12-SM, d17:1-S1P, d17:1-Sph, C8-GluCer, C8-GalCer, C8-LacCer, Gb3-d18:1/17:0, d3-16:0 carnitine, DAG(17:0/17:0)-d5 were obtained from Avanti Polar Lipids. GM3-d18:1/18:0-d3 was purchased from Matreya LLC. Free fatty acids were quantitated using d31-16:0

(Sigma-Aldrich). d6-CE 18:0 and TAG(16:0)3-d5 were obtained from CDN isotopes.

Statistical analysis

Data are presented as the mean \pm standard deviations. Statistical significance was performed using one-way analysis of variance with two-tailed t-test method and two-sample heteroscedasticity. Graphs and statistical results were generated in GraphPad Prism (version 9.5.1). Group differences between means were considered statistically significant for $P < 0.05$ (*).

Results

Upregulation of TMEM68 in breast cancer patients is associated with poor survival

Compared with normal breast tissues, the *TMEM68* gene was upregulated in bulk breast cancer tissues (Fig. 1A). However, this upregulation did not significantly vary across cancer stages (Fig. 1B). Higher *TMEM68* gene expression was correlated with a decrease in OS and DFS, as shown by GEPIA (Fig. 1C, D). Similarly, compared to breast cancer patients with low *TMEM68* levels, the probabilities of DFI and MFS were significantly lowered in those with high *TMEM68* expression (Fig. 1E and F). IHC staining showed elevated *TMEM68* protein expression in breast tumor tissue relative to normal breast tissue (Fig. 1G). These analyses suggest that *TMEM68* may contribute to breast cancer pathogenesis.

Effect of TMEM68 on breast cancer cell proliferation, migration and invasion

TMEM68 expression was firstly analyzed in four breast cancer cell line subtypes. *TMEM68* gene expression was highest in luminal B BT-474 cells, followed by luminal A MCF-7 cells, and relatively lower in both SK-BR-3 (HER2-positive) and MDA-MB-453 (TNBC) cells (Fig. S2A). Immunoblotting analysis revealed a similar trend at the protein levels (Fig. S2B). Thus, *TMEM68* is differentially expressed across distinct breast cancer cell subtypes.

Based on the expression profiles, MCF-7 and SK-BR-3 cells were selected for overexpression experiments, whereas MCF-7 and BT-474 cells were used for knockdown assessments. In *TMEM68* overexpressing SK-BR-3/*TMEM68* and MCF-7/*TMEM68* cells, *TMEM68* mRNA levels increased by approximately 12- and 30-fold, respectively, compared with control cells (Fig. S3). Conversely, compared with the scrambled shRNA (shControl), *TMEM68* knockdown by shRNA (sh*TMEM68*) significantly reduced *TMEM68* mRNA levels by >80% in both MCF-7 and BT-474 cells (Fig. S3).

Beginning at 24 h post seeding, cell proliferation rates were monitored through comparing the CCK-8 absorbance values at different times. Overexpression of

TMEM68 promoted the growth of MCF-7 and SK-BR-3 cells at 72 and 96 h post seeding (Fig. 2A and B). Conversely, *TMEM68* knockdown markedly inhibited MCF-7 cells but not in BT-474 cell proliferation (Fig. 2C and D). Thus, *TMEM68* overexpression enhances breast cancer cell proliferation, whereas *TMEM68* knockdown inhibits this process in cell dependent manner.

In addition, transwell migration assays without matrigel showed that overexpression of *TMEM68* promoted MCF-7, but not SK-BR-3 cells migration, while *TMEM68* knockdown did not affect cell migration in both MCF-7 and BT-474 cells (Fig. 2E and G). Next, transwell invasion assays with matrigel revealed that enhanced *TMEM68* expression improved MCF-7 and SK-BR-3 cells invasion, conversely knockdown of *TMEM68* has no impact on cell invasion in both MCF-7 and BT-474 cells (Fig. 2F and H).

TMEM68 controls TAG levels and LD content in breast cancer cells

Consistent with previous results [25, 26], overexpression of *TMEM68* increased TAG levels by approximately 3.2- and 2.1-fold compared with control MCF-7 cells under both basal conditions and OA supplementation conditions, respectively (Fig. 3A). Similarly, *TMEM68* overexpression in SK-BR-3 cells elevated TAG levels by more than 2.2-fold, both with and without OA supplementation (Fig. 3A). In contrast, *TMEM68* knockdown reduced TAG levels by more than 20% reduction in both MCF-7 and BT-474 cells, with or without OA loading (Fig. 3B).

As synthesized TAGs are stored in the core of LDs, the impact of *TMEM68* on LDs was investigated. As shown in Fig. 3C, MCF-7/*TMEM68* cells accumulated larger and more numerous LDs compared with control MCF-7 cells, whereas *TMEM68* knockdown in sh*TMEM68*-expressing cells resulted in fewer dispersed LDs compared with shControl-expressing cells (Fig. 3C). Oil Red O staining confirmed that *TMEM68* overexpression and knockdown elevated and reduced intracellular neutral lipid accumulation, respectively, under both basal and OA-supplemented conditions (Fig. S4). These findings indicate that *TMEM68* regulates TAG levels and LD content in breast cancer cells.

To further understand how *TMEM68* influences global lipid profiles, quantitative lipidomic analysis was performed on *TMEM68* overexpression and knockdown MCF-7 cells, along with their control cells. The lipid species analyzed included glycerolipids, glycerophospholipids (GPLs), fatty acyls, sphingolipids and sterols, with TAG comprising 37% of the lipid species number (Supplementary Tables 2 and 3). Heatmap analysis revealed that *TMEM68* expression markedly altered the levels of various lipids (Fig. S5). In particular, *TMEM68* overexpression significantly increased TAG levels by more than 5.5-fold compared with MCF-7 control cells (Fig. 4A),

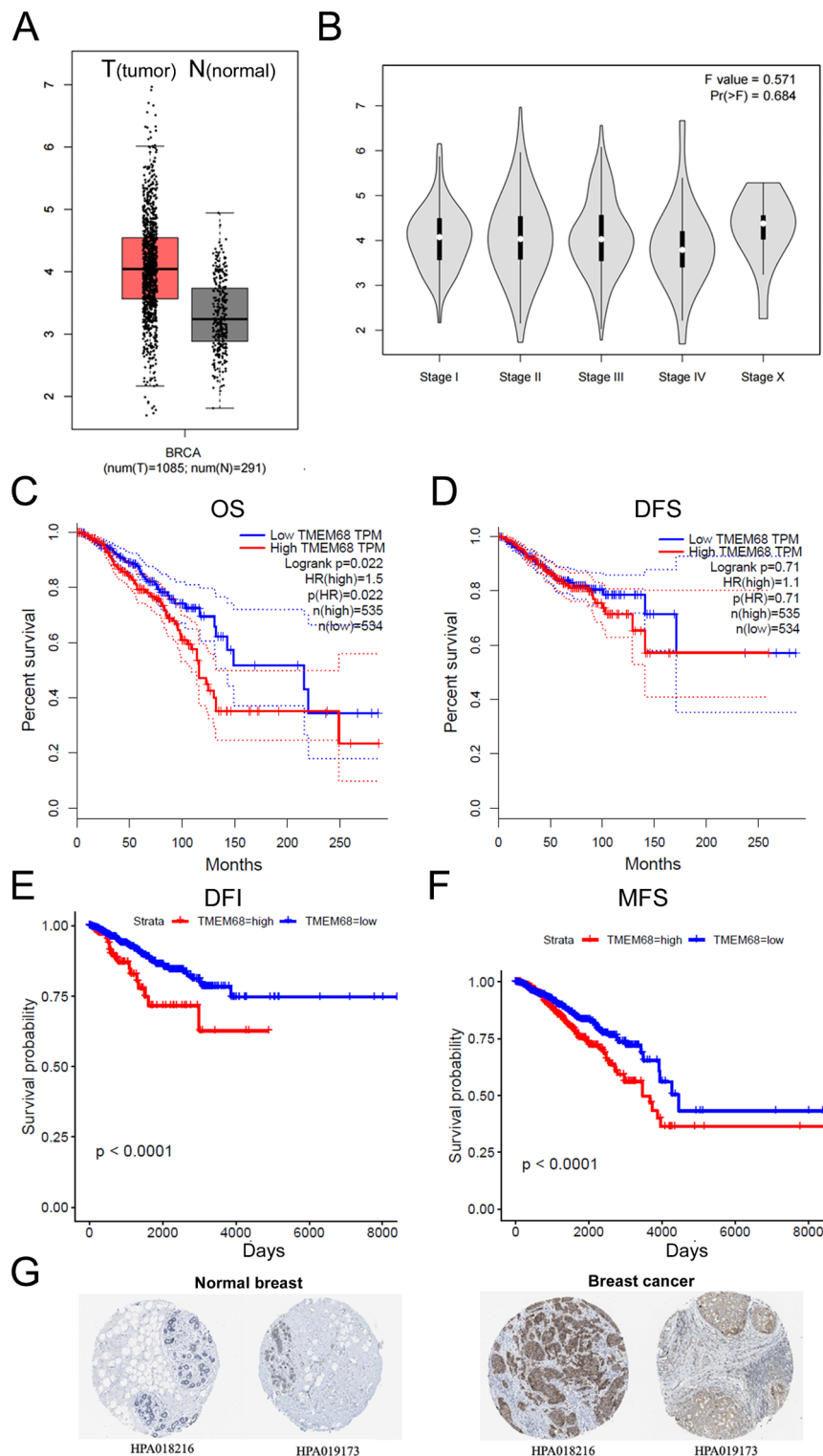


Fig. 1 Expression profiling and survival analysis of *TMEM68* gene in breast cancer. **A** and **B**, Comparisons the expression of *TMEM68* gene between para-cancerous normal tissues and breast cancer tissues depicted with box plots (**A**) and stage plots (**B**). Each dot represents an individual cancer or normal sample. **C-F**, Survival analysis of patients stratified by low (blue line) or high (red line) *TMEM68* gene expression, including OS (overall survival) (**C**), disease-free survival (DFS) (**D**), disease-free interval (DFI) (**E**) and metastasis-free survival (MFS) (**F**). **G**, Representative images of immunohistochemical staining for *TMEM68* in normal and cancerous breast tissues

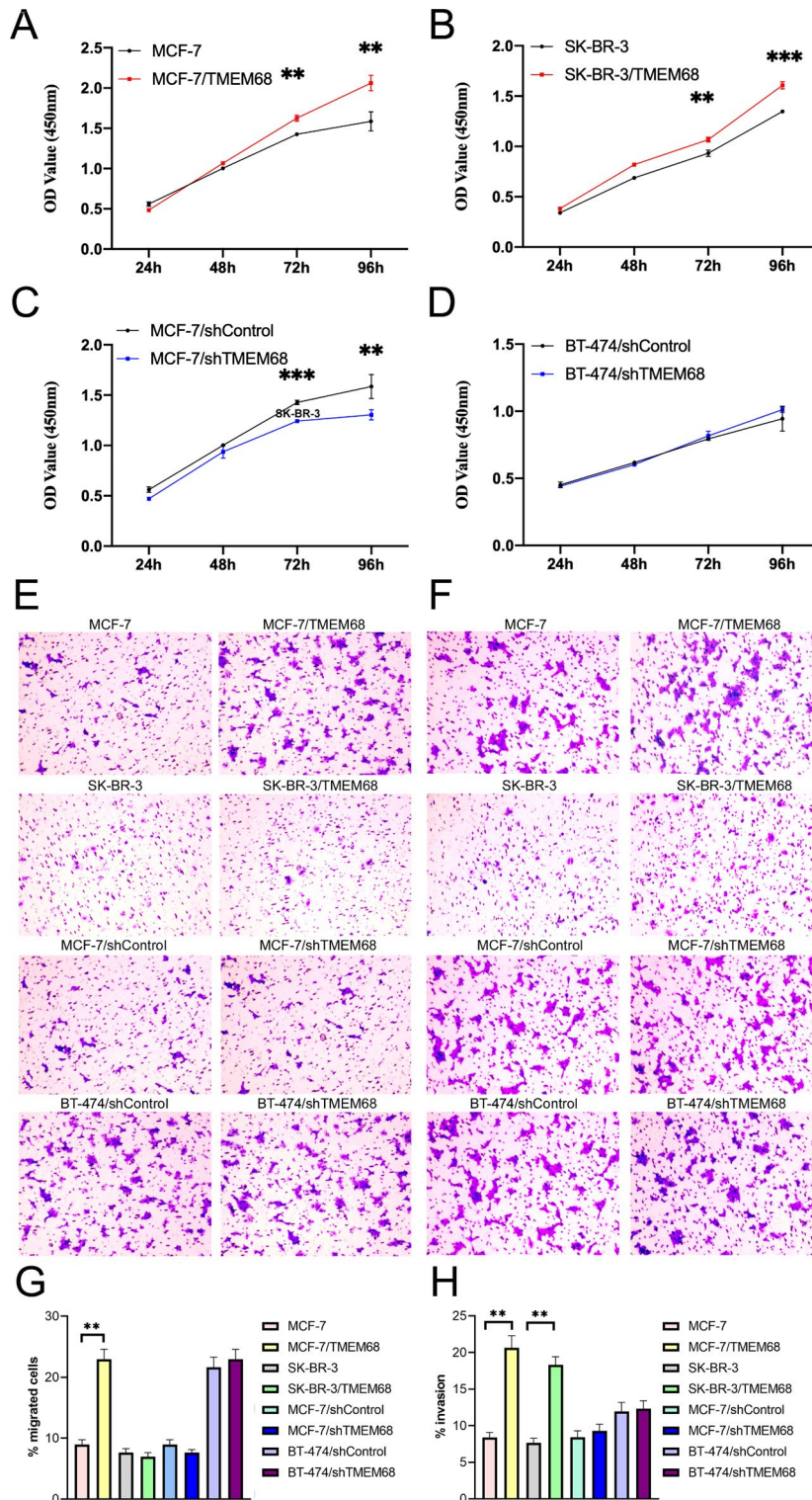


Fig. 2 Impact of TMEM68 expression on breast cancer cell proliferation, migration and invasion. **A-D**, Cells were seeded into 96-well plates, and cell viability was determined at the indicated post-seeding times by measuring absorbance at 450 nm using the CCK-8 kit assay. $n=4$. **E**, Transwell migration assay towards 20% FBS. Representative micrographs (20 \times) were taken from the membrane filter (bottom surface of filters) stained with Crystal violet. **F**, Transwell matrigel invasion assay towards 20% FBS. **G** and **H**, Quantification of transwell migration (**G**) and matrigel invasion (**H**) assay by counting the number of cells present in the lower compartment, $n=3$. Data are presented as the means \pm SDs. Asterisks indicate P values: ** $P < 0.01$, *** $P < 0.001$

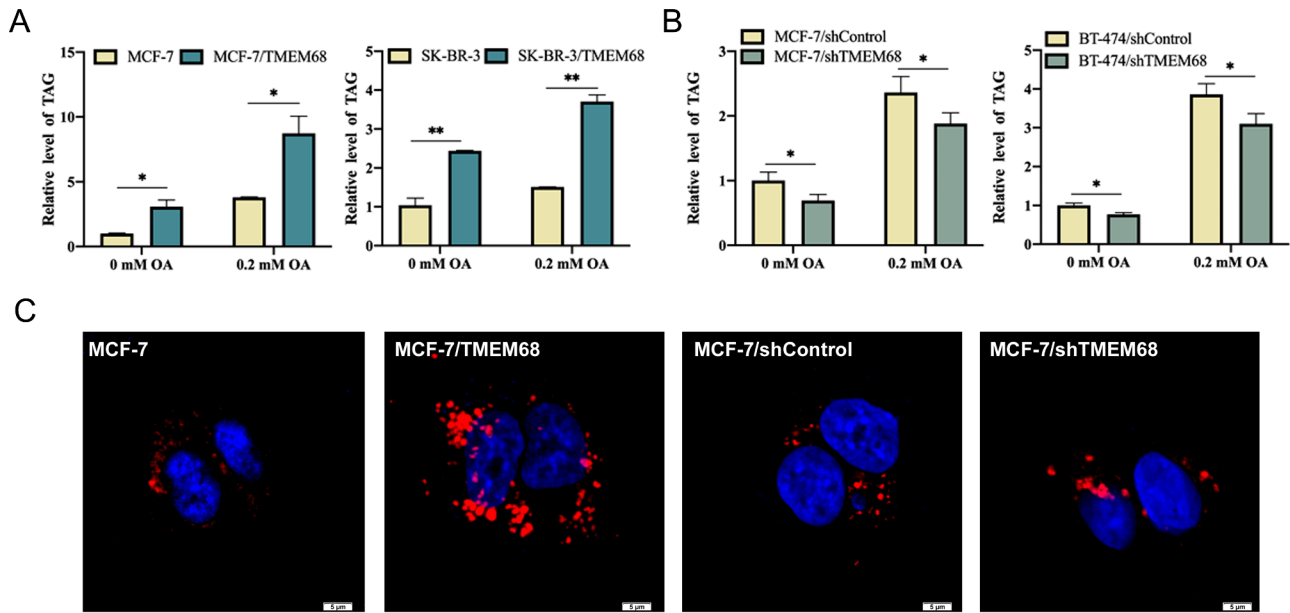


Fig. 3 TMEM68 regulates TAG levels and LD content in breast cancer cells. **A** and **B**, Relative TAG levels were in TMEM68 overexpression (**A**) and knock-down (**B**) cells incubated with OA or not. Data are presented as the means \pm SDs. Asterisks indicate *P* values: * $P < 0.05$, ** $P < 0.01$, $n = 4$. **C**, LD and nuclei were stained with LipidTOX™ Deep Red and DAPI, respectively. Images were captured by laser confocal microscopy. Scale bars = 5 μ m

whereas TMEM68 knockdown reduced TAG levels by approximately 20% (Fig. 4B). Additionally, the levels of MAG and DAG, precursors in TAG synthesis, were elevated 2.1- and 2.5-fold, respectively, by TMEM68 overexpression (Fig. 4A), although they were not affected by TMEM68 knockdown (Fig. 4B). TMEM68 overexpression specifically promoted the accumulation of MAG species, such as MAG 14:1 and MAG 16:1 (Fig. 4C). Furthermore, TMEM68 overexpression led to an increase in 18 out of 26 DAG species, most of which contained saturated and monounsaturated fatty acids (SFAs, MUFAs), with nonsignificant increases in polyunsaturated fatty acids (PUFAs) (Fig. 4D). A heatmap analysis showed that nearly all TAG species were elevated in TMEM68 overexpression cells (Fig. S6A), with the contents of all TAG subclasses, regardless of fatty acid saturation (C=C bond) being elevated (Fig. 5A). Notably, 30 TAG species, most containing SFAs and MUFAs, were upregulated by >10-fold, with TAG46:3 (16:1) and TAG48:3 (16:1) increased by >40-fold (Fig. 5B). In contrast, TMEM68 knockdown led to a reduction in most TAG species, as shown in the heatmap (Fig. S6B), with 21 TAG species showing more than a 50% reduction, many of which contained PUFAs (Fig. 5C). Collectively, these findings demonstrated that TMEM68 is a key regulator of TAG abundance in breast cancer cells.

TMEM68 alters glycerophospholipid composition in breast cancer cells

GPLs are essential components of the cancer cell membrane. The impact of TMEM68 on various GPL levels

was examined in MCF-7 cells. TMEM68 overexpression increased levels of total phosphatidylethanolamine (PE) by 1.25-fold and phosphatidic acid (PA), an intermediate metabolite in the G3P pathway, by 1.8-fold (Fig. 6A). Specifically, all 13 PA species analyzed were elevated (Fig. 6C). However, the content of 1-O-alkyl-2-acylphosphatidylcholine (PC-O) was reduced by 21.7% due to TMEM68 overexpression (Fig. 6A). Knockdown of TMEM68 similarly reduced PC-O levels by 21.3%, while increasing PA and phosphatidylglycerol (PG) contents by 1.7- and 1.8-fold, respectively (Fig. 6B). Among the 13 PA species examined, 10 showed increased levels (Fig. 6D). Regarding lysophospholipids, TMEM68 overexpression decreased the content of lysophosphatidic acid (LPA), the first intermediate metabolite in the G3P pathway, by 18.6% (Fig. 6E). Among the four LPAs examined, two LPAs containing PUFAs showed decreased levels, whereas those with SFAs remained unaffected (Fig. 6F). Additionally, lysophosphatidylcholine (LPC) levels were reduced by 23% in TMEM68-knockdown cells (Fig. 6G), with significant decreases observed in 12 LPC species (Fig. 6H). Collectively, TMEM68 broadly influences GPL metabolism in breast cancer cells.

TMEM68 potentially mediates an alternative TAG synthesis pathway possibly using GPLs, especially PC and ether-linked PC (ePC), as fatty acid donors [26]. Hence, PC and ePC compositions were analyzed. Overexpression of TMEM68 reduced the levels of 23 out of 25 PC-O species examined (Fig. 7A). Although total PC content was not altered by TMEM68 overexpression, heatmap analysis revealed a downregulation in

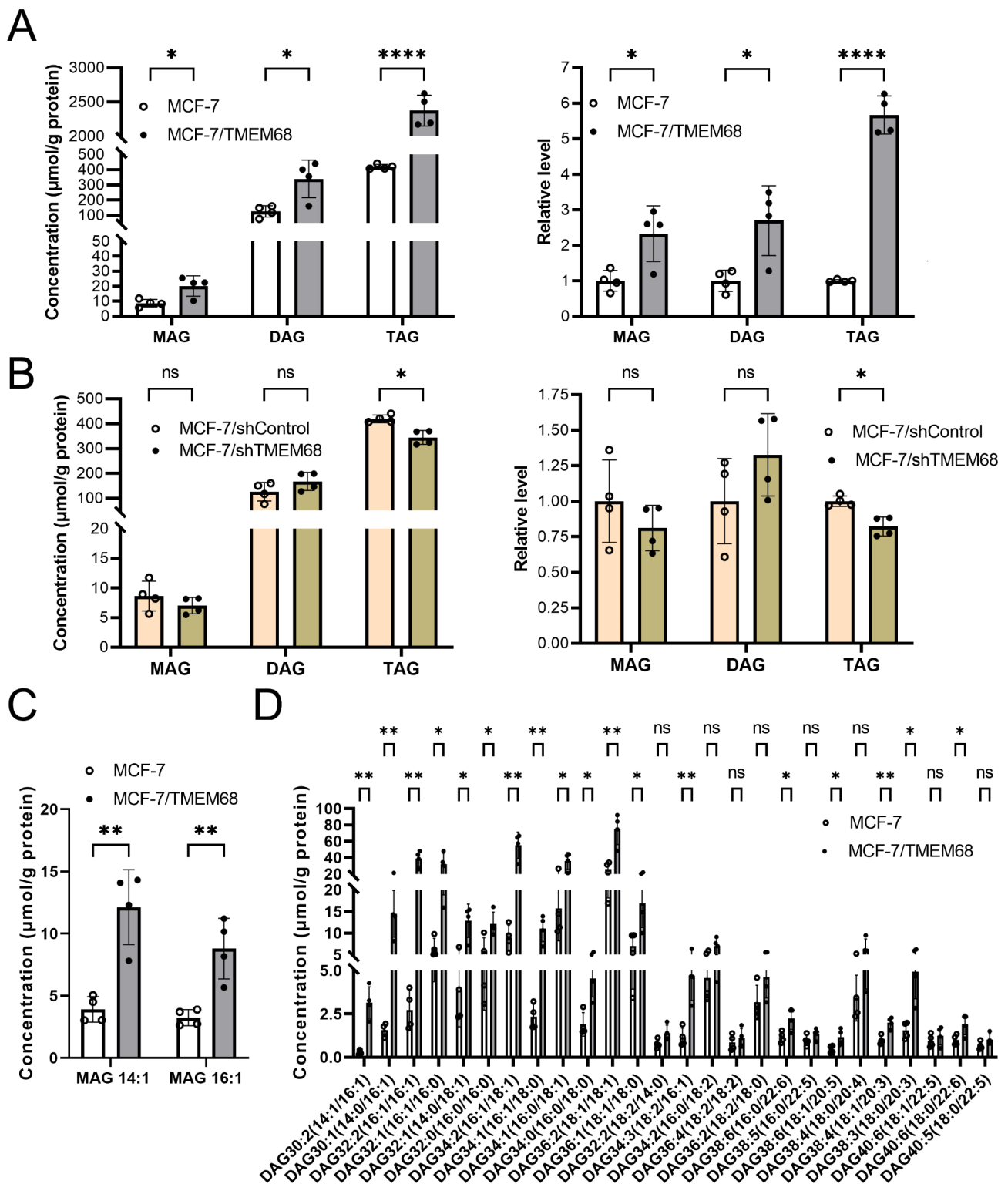


Fig. 4 TMEM68 expression altered the intracellular glycerolipids levels. **A** and **B**, Concentrations and relative levels of total MAG, DAG and TAG in MCF-7/TMEM68 and MCF-7 cells (**A**), MCF-7/shTMEM68 and MCF-7/shControl cells (**B**). **C** and **D**, Levels of MAG (**C**) and DAG (**D**) species in MCF-7/TMEM68 and MCF-7 cells. Data are expressed as means \pm SDs ($n=4$). Asterisks indicating P values. * $P < 0.05$, ** $P < 0.01$, **** $P < 0.0001$. ns, not significant

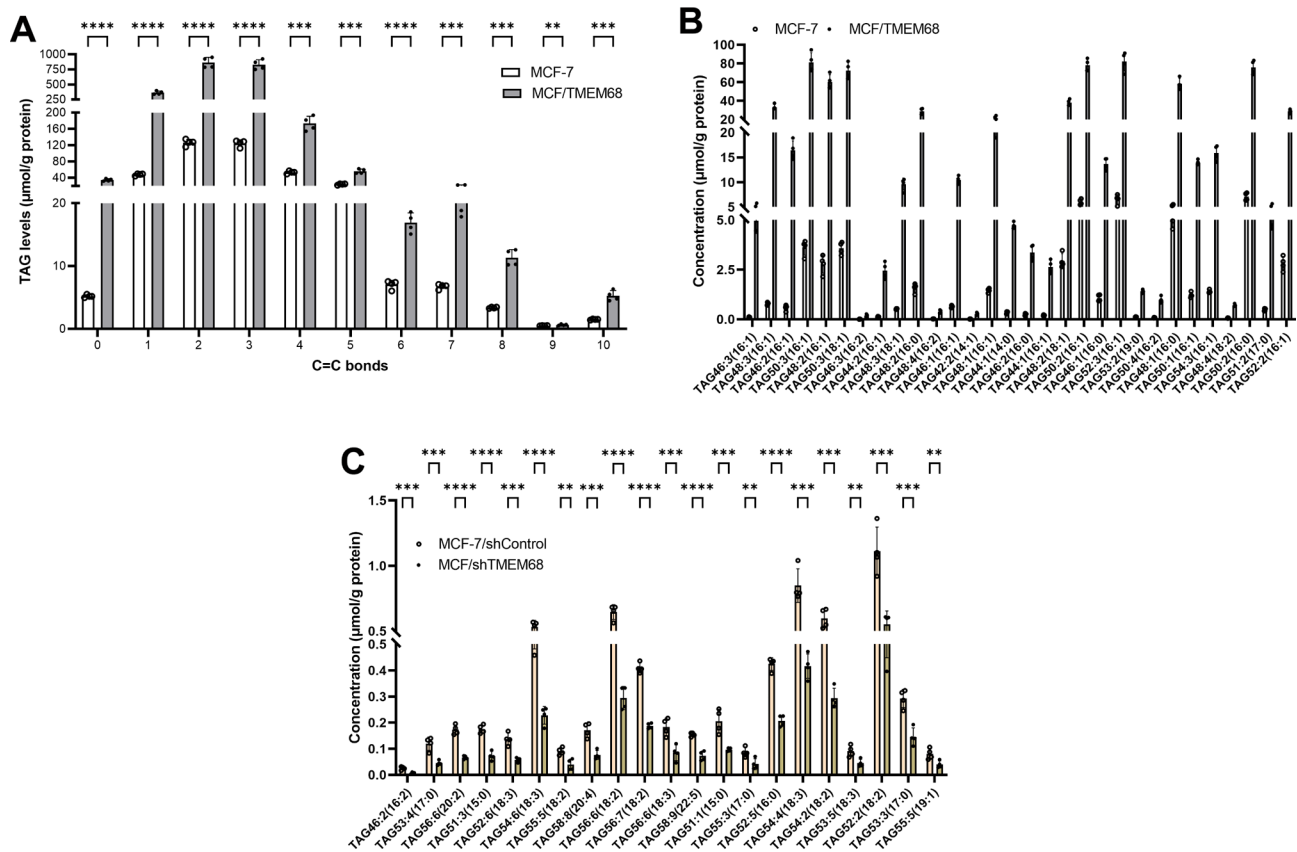


Fig. 5 TMEM68 expression affected TAG content in breast cancer cells. **A**, Levels of TAG containing different saturations in MCF-7/TMEM68 and MCF-7 cells. **B**, TAG species contents between MCF-7/TMEM68 and MCF-7 cells with the increased fold change ≥ 10 . **C**, TAG levels between MCF-7/shTMEM68 and MCF-7/shControl cells with a reduced fold change ≤ 0.50 . Data are presented as the means \pm SDs. Asterisks indicating *P* values. ** *P* < 0.01, *** *P* < 0.001, **** *P* < 0.0001. ns, not significant. All *P* < 0.0001 in B. *n* = 4

PC species with unidentified fatty acids on the glycerol backbone, especially those containing more than three C=C bonds (Fig. 7B). TMEM68 overexpression did not noticeably affect the total amount of PCs containing two defined fatty acids (PC-FAs) (Fig. 7C). However, the relative abundance of PCs with PUFAs at the *sn*-2 position decreased significantly, despite the abundance of PCs with *sn*-2 SFAs and MUFAs increasing (Fig. 7D). Notably, TMEM68 knockdown similarly reduced nearly all PC-O species contents (Fig. 7E). Collectively, TMEM68 markedly affects PC and ePC compositions in breast cancer cells.

TMEM68 modulates sterol lipid and acylcarnitine levels

Overexpression of TMEM68 significantly increased total CEs levels by approximate 1.8-fold (Fig. 8A). Specifically, 2 out of 6 detected CE species contents were significantly elevated, however the other three increased CEs appeared to be non-significant due to individual variability (Fig. 8B). Conversely, TMEM68 knockdown did not affect total CE levels (Fig. 8C). Among the fatty acyls, acylcarnitine content was reduced by 44% due to TMEM68 overexpression (Fig. 8D), with reductions in 3

out of 4 acylcarnitine species containing saturated and unsaturated fatty acyls (Fig. 8E). Conversely, no significant changes in acylcarnitine levels were observed following TMEM68 knockdown (Fig. 8F).

TMEM68 affects the expression of genes involved in lipid metabolism

To investigate how TMEM68 influences lipid metabolism, the expression of genes encoding key enzymes involved in lipid metabolism, especially in TAG metabolism, was analyzed. Despite the accumulation of TAG, TMEM68 overexpression did not affect mRNA levels of *DGAT1* or *DGAT2* genes (Fig. 9A). However, TMEM68 knockdown decreased the expression of *DGAT1*, but not the *DGAT2* gene. The genes for two key enzymes in TAG mobilization, *ATGL* and hormone-sensitive lipase (*HSL*), which hydrolyze TAG and DAG, respectively [19], were also examined. Although TMEM68 had no effect on *ATGL* expression, TMEM68 overexpression and knockdown led to upregulated and downregulated *HSL* expression, respectively.

In addition, TMEM68 overexpression and knockdown upregulated the expression of the genes related to

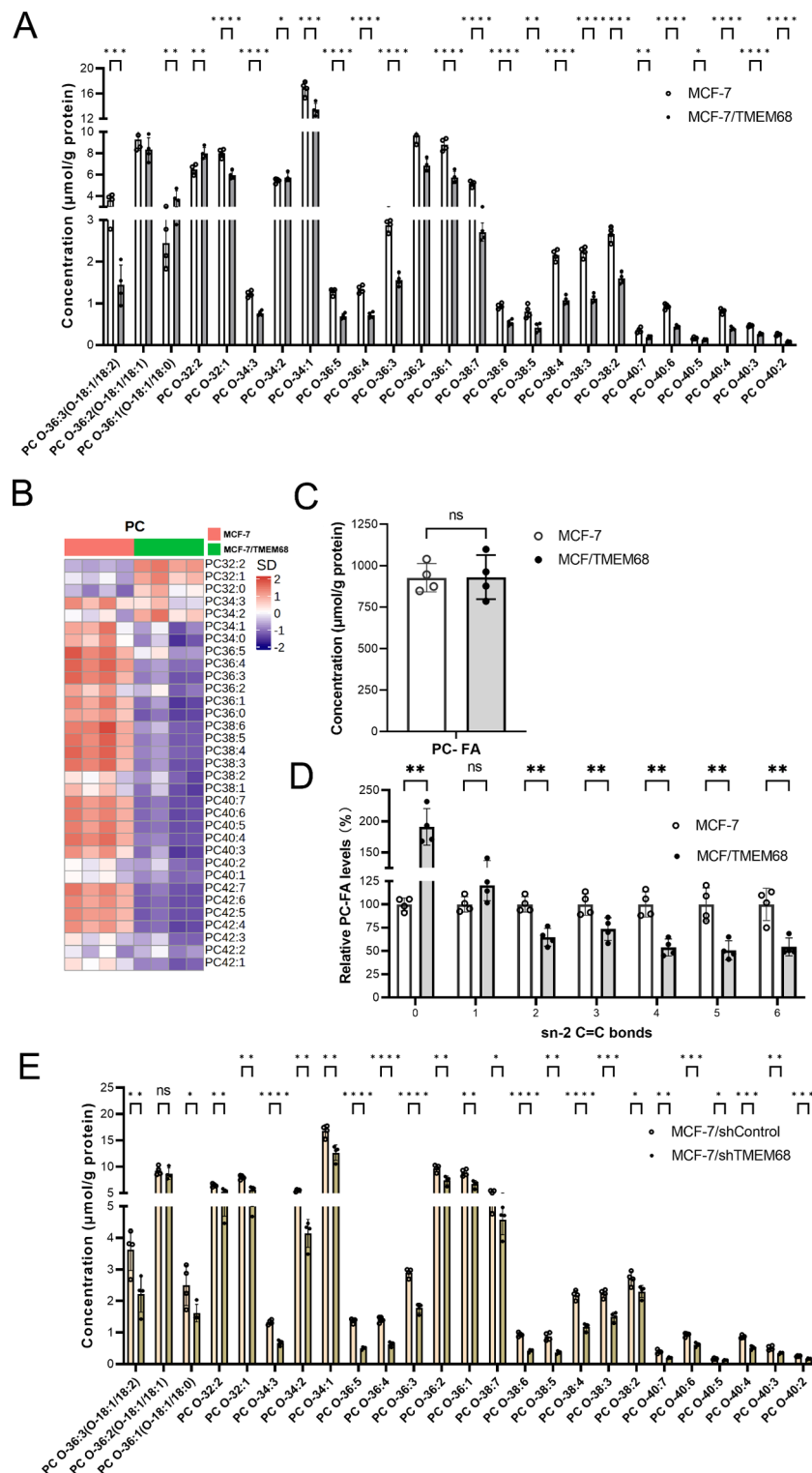


Fig. 7 TMEM68 affected PC and ether-PC composition. **A** and **E**, Comparison of PC-O species levels between MCF-7 and MCF-7/TMEM68 cells (**A**), between MCF-7/shTMEM68 and MCF-7/shControl cells (**E**). **B**, Heatmap analysis of PC species with undefined fatty acids between MCF-7 and MCF-7/TMEM68 cells. **C** and **D**, Comparisons of total PC-FAs (**C**) and PC-FA with different saturated fatty acids at *sn*-2 position (**D**) levels between MCF-7 and MCF-7/TMEM68 cells. Data are presented as the means \pm SDs. Asterisks indicates *P* values. * $P < 0.05$, ** $P < 0.01$, *** $P < 0.001$, **** $P < 0.0001$. ns, not significant, $n = 4$

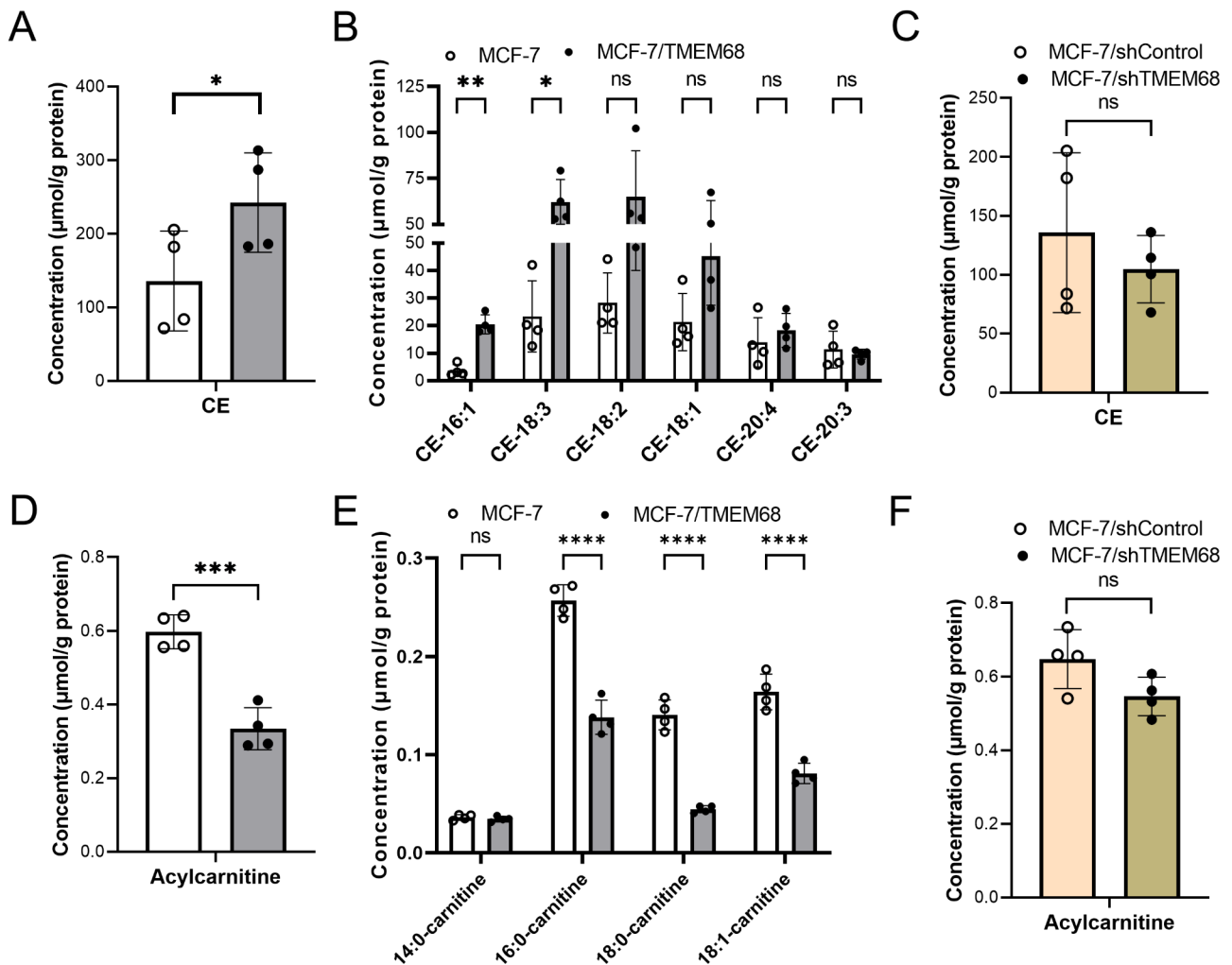


Fig. 8 TMEM68 altered CE and acylcarnitine levels in breast cancer cells. **A, C, D** and **F**, Comparison of total CEs (**A, C**) and acylcarnitines (**D, F**) between MCF-7 and MCF-7/TMEM68 cells (**A, D**), between MCF-7/shControl and MCF-7/shTMEM68 cells (**C, F**). **B** and **E**, Contents of CEs (**B**) and acylcarnitine (**E**) in MCF-7 and MCF-7/TMEM68 cells. The data are presented as the means ± SDs. Asterisks indicates *P* values. * *P* < 0.05, ** *P* < 0.01, *** *P* < 0.001, **** *P* < 0.0001. ns, not significant, *n* = 4

fatty acid synthesis, including acetyl-CoA carboxylase α (ACACA), fatty acid synthase (FASN) and stearoyl-CoA desaturase 1 (SCD1). Owing to an increase in CEs observed with TMEM68 overexpression, the mRNA levels of sterol-O-acyltransferase (SOAT), *SOAT1* and *SOAT2*, encoding key enzymes responsible for CE synthesis [34], were measured. The expression of *SOAT2*, but not *SOAT1* gene, was upregulated by TMEM68 overexpression and downregulated by TMEM68 knock-down. Furthermore, the expression of two transcription factors involved in lipogenesis, peroxisome proliferator-activated receptor γ (PPARγ) and PPARα was quantified. The expression of *PPARγ*, but not *PPARα* gene was upregulated by TMEM68 overexpression and knock-down (Fig. 9A, B). GPAT is the rate-limiting enzyme in the G3P pathway for TAG synthesis [18]. Overexpression and knockdown of TMEM68 both upregulated the

mRNA levels of most GPAT genes, including *GPAT2*, *GPAT3* and *GPAT4* (Fig. 9C, D). Finally, the impact of TMEM68 on the expression of *TMX1*, a potential suppressor of TMEM68 activity was determined. TMEM68 overexpression significantly increased *TMX1* mRNA levels, whereas TMEM68 knockdown had no effect (Fig. 9E, F). These findings show that TMEM68 modulates the expression of key genes responsible for TAG and CE metabolism.

Discussion

TMEM68 is a potential modifier of breast cancer risk and outcomes in humans, and the *TMEM68* gene is expressed at higher levels in susceptible mammary tumors compared with resistant mammary tumors in rats [27]. In the current study, GEPIA and IHC staining confirmed that TMEM68 were increased at mRNA and protein

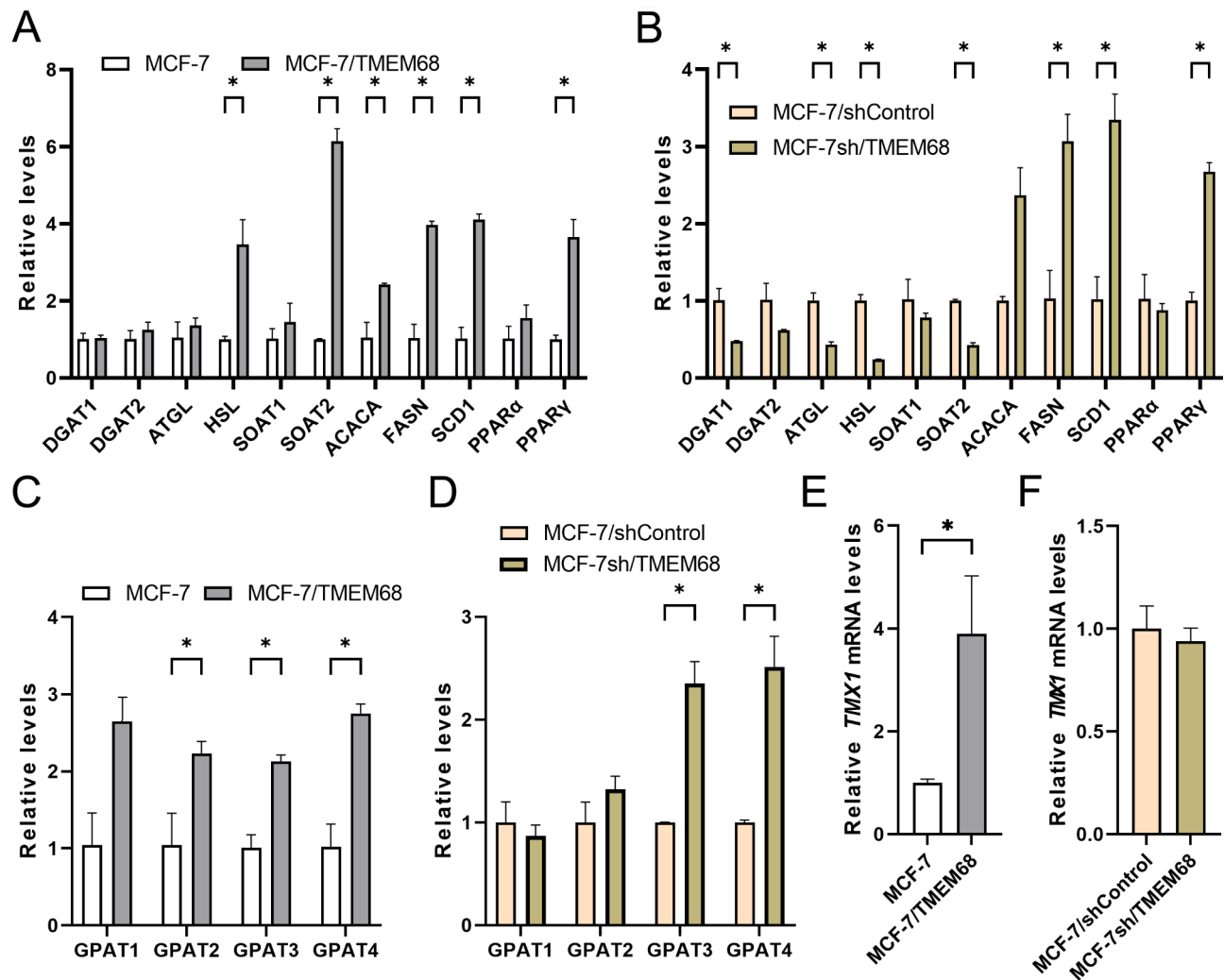


Fig. 9 TMEM68 altered the expression of genes related to lipid metabolism. Total RNA was extracted and then reverse transcribed to cDNA. mRNA levels were quantified by qPCR and normalized to the expression of β -actin gene. The results are presented as the fold change relative to the control cells. Data are presented as the means \pm SDs. Asterisks indicates *P* values. * *P* < 0.05, *n* = 4

levels in breast cancer tissues relative to normal breast tissues. Survival analysis also indicated that high levels of TMEM68 were associated with reduced OS, DFS, DFI, and MFS in breast cancer patients. These analyses suggest that TMEM68 may function in the pathogenesis of breast cancer.

Functionally, TMEM68 acts as an DGAT-independent acyltransferase, synthesizing TAG using DAG as an acceptor of fatty acyls, and its overexpression promotes LD accumulation in mammalian cells [25, 26]. Here, TMEM68 overexpression significantly increased TAG levels in two breast cancer cell lines, whereas TMEM68 knockdown led to an approximate 20% reduction in TAG content. Despite these changes in TAG levels, TMEM68 overexpression did not alter the expression of *DGAT1* and *DGAT2* gene, encoding the final enzymes in canonical TAG synthesis pathways [17, 18]. *TMX1* was demonstrated to be associated with TMEM68 as a potential

TMEM68 activity suppressor [26]. The expression of *TMX1* gene was upregulated due to TMEM68 overexpression, which may be a feedback inhibitory mechanism to maintain TAG hemostasis. However, TMEM68 knockdown did not alter *TMX1* expression, and resulted in decreased *DGAT1*, but not *DGAT2* mRNA levels, which potentially contributes to the observed reduction in TAG content.

Hydrophobic TAG is stored in the LD core surrounded by a monolayer of phospholipids [16]. Increased TAG levels led to LD accumulation in TMEM68-expressing MCF-7 cells. Such LD accumulation is a hallmark of cellular carcinogenesis [8], as LDs abundance is positively correlated with breast cancer progression and promotes cancer cell growth and survival [9, 12]. Therefore, changes in TAG levels and LD content driven by TMEM68 expression may play a role in the regulation of breast cancer cell proliferation.

TMEM68 expression varied across different breast cancer cell subtypes. TMEM68 overexpression significantly promoted cell growth in luminal A MCF-7 and HER2-positive SK-BR-3 cells, both of which showed relatively low endogenous TMEM68 levels. These findings align with the observation of higher TMEM68 levels in human breast cancer and rat susceptible mammary tumors compared with normal breast tissues and resistant mammary tumors, respectively [27]. Conversely, silencing TMEM68 had only a modest impact on MCF-7 cell proliferation and no impact on BT-474 Lumina B cells, which have relatively higher endogenous TMEM68 levels. Given the several-fold increase in TAG levels with TMEM68 overexpression and the 20% reduction with its knockdown, the impact of TMEM68 on cell proliferation may be closely associated with its effect on TAG metabolism in breast cancer cells.

In addition to TAG, CEs accumulated with TMEM68 overexpression and decreased with TMEM68 knockdown in breast cancer cells, consistent with findings in other cells [25, 26]. The regulation of CEs levels appeared to involve the upregulation and downregulation of *SOAT2* (but not *SOAT1*) due to overexpression and knockdown of TMEM68, respectively. Fatty acyl-CoA, activated from free fatty acids, can be used not only for TAG and CE synthesis, but also for the formation of acylcarnitine for mitochondrial energy production [35, 36]. The reduction in acylcarnitine levels observed with TMEM68 overexpression may represent an adaptive response supporting increased TAG and CE accumulation.

TMEM68 represents a distinct subgroup within the glycerophospholipid acyltransferases, exhibiting a substantial phylogenetic divergence from other members, such as GPAT and AGPAT enzymes involved in the G3P pathway for TAG synthesis [23]. TMEM68 does not contain binding motifs conserved in GPAT and AGPAT [24], suggesting that it may have unique acyltransferase activity. Overexpression of TMEM68 has been shown to increase TAG levels in a DGAT-independent manner [25, 26]. This increase in TAG is potentially due to the acyltransferase activity of TMEM68, which likely incorporates fatty acyl groups from PC and ePC, rather than from acyl-CoA, into DAG for TAG synthesis [26]. Lipidomic analysis revealed that although total PC levels were not significantly reduced, most PC species containing more total C=C bonds fatty acids and PUFAs at the *sn*-2 position tended to show decreased levels. In contrast, PC molecules with SFAs and MUFAs levels exhibited increased levels with TMEM68 overexpression. Ether lipids make up approximately 20% of the total phospholipid content in mammalian biological membranes [37]. In nature ether glycerophospholipids are often found in PC and PE species [38]. In the present study, levels of PC-O, an ether-linked PC form, were decreased significantly by

TMEM68 overexpression. Additionally, TMEM68 overexpression increased DAG content. Notably, levels of DAGs species containing SFAs and MUFAs were significantly elevated, whereas most DAG species with PUFAs showed no significant change. These alterations in DAG, PC and PC-O may together lead to an increase in levels of nearly all TAGs, particularly containing SFAs and MUFAs.

PA is the direct precursor of DAG synthesis in the G3P pathway [17, 18], and its elevated levels in TMEM68-overexpressing cells implied that enhanced DAG synthesis occurred through this pathway. This was further supported by the upregulation of several *GPAT* gene due to TMEM68 overexpression. DAG also serves as a precursor for the synthetic of PC, phosphatidylserine (PS) and PE in the Kennedy pathway [39]. Typically, PC synthesized through the Kennedy pathway usually contains SFAs and MUFAs on the glycerol backbone [38]. The PUFAs at the *sn*-2 position is remodeled by the Lands' cycle, which involves phospholipase As (PLAs) and lysophospholipid acyltransferases (LPLATs) [40, 41]. Given that mammalian cells can synthesize SFAs and MUFAs, but not PUFAs due to the absence of specific desaturases [42], the reduction in PC species containing *sn*-2 PUFAs could not be compensated, leading to an increase in PCs containing SFAs and MUFAs. Increased levels of PAs and DAGs may reflect a feedback mechanism responding to TMEM68 overexpression. Depletion of DAG and PC to drive TAG synthesis further supports the role of TMEM68 in using PC as an acyl donor for TAG synthesis. In contrast, TMEM68 knockdown led to an approximate 20% reduction in TAG levels without affecting DAG content. This reduction in TAG could not be compensated by DGAT enzymes, despite increased PA levels in TMEM68-deficient cells. PA also serves as a precursor of phosphatidylinositol (PI), PG, and cardiolipin (CL) synthesis through the cytidine diphosphate–DAG pathway [39], with PA accumulation leading to increased PG levels. Thus, TMEM68 plays a crucial role in basal cellular glycerophospholipid remodeling.

Strengths and limitations

This study provided a comprehensive analysis of TMEM68 expression profiles and multiple survival outcomes in breast cancer. It was the first time to examine TMEM68 expression across different breast cancer subtypes and to clarify its role in cell proliferation. This study also explored the effects of TMEM68 on lipid metabolism using an unbiased lipidomic analysis method, providing insights into the potential biochemical mechanisms in breast cancer cells.

The limitations were as follows: (1) the role of TMEM68 in cell growth, migration and invasion was preliminarily elucidated, without investigating more key

carcinogenic processes, such as apoptosis; (2) the impact of TMEM68 on cell proliferation was not demonstrated in a mouse tumorigenesis model; and (3) further clarification is required on how TMEM68-driven changes in lipid metabolism, especially in TAG homeostasis, regulate breast cancer cell proliferation.

Conclusions

In conclusion, TMEM68 is upregulated in patients with breast cancer, with higher levels associated with poorer survival outcomes. TMEM68 overexpression significantly promotes the proliferation of breast cancer cells, whereas its knockdown has a less pronounced impact. TMEM68 modulates TAG levels and LD content, along with changes in DAG and glycerophospholipid compositions, particularly PC and ePC contents. Thus, TMEM68 may function as a potential regulator of breast cancer cell growth through lipid metabolism reprogramming. The expression level of TMEM68 may be used to predict the survival outcome of breast cancer patients, as well as the inhibition efficiency of drugs targeting TMEM68 on breast cancer cell proliferation.

Abbreviations

ACACA	Acetyl-CoA carboxylase α
AGPAT	Acylglycerolphosphate acyltransferase
ATGL	Adipose triglyceride lipase
CE	Cholesteryl ester
DAG	Diacylglycerol
DFI	Disease-free interval
DFS	Disease-free survival
DGAT	Acyl-CoA: diacylglycerol acyltransferase
ePC	Ether-linked PC
ER	Endoplasmic reticulum
FASN	Fatty acid synthase
FFA	Free fatty acid
G3P	Glycerol 3-phosphate
GEPIA	Gene expression profiling interactive analysis
GPAT	Glycerol-3-phosphate acyltransferase
GPLs	Glycerophospholipids
HSL	Hormone-sensitive lipase
IHC	Immunohistochemistry
LD	Lipid droplet
LPA	Lysophosphatidic acid
MAG	Monoacylglycerol
MFS	Metastasis-free survival
MGAT	Monoacylglycerol acyltransferase
MUFA	Monounsaturated fatty acid
OS	Overall survival
PA	Phosphatidic acid
PC	Phosphatidylcholine
PE	Phosphatidylethanolamine
PG	Phosphatidylglycerol
PMSF	Phenylmethanesulfonyl fluoride
PPAR	Peroxisome proliferator-activated receptor
PS	Phosphatidylserine
PUFA	Polyunsaturated fatty acid
SCD1	Stearoyl-CoA desaturase 1
SFA	Saturated fatty acid
SOAT	Sterol-O-acyltransferase
TAG	Triacylglycerol
TMEM68	Transmembrane protein 68

Supplementary Information

The online version contains supplementary material available at <https://doi.org/10.1186/s12944-024-02369-6>.

Supplementary Material 1
Supplementary Material 2
Supplementary Material 3
Supplementary Material 4
Supplementary Material 5

Acknowledgements

Not applicable.

Author contributions

Z. Z., Q. Y. and F. Z. performed experiments, data collection, data analysis. X. H. and Q. S. reviewed and proofread the manuscript. H. P. performed data analysis and edited the manuscript. P. C. conceptualized this project, supervised the overall work and wrote the manuscript. All authors read and approved the final manuscript.

Funding

This work is supported by grants from the Chongqing Science and Technology Bureau (No. CSTB2022NSCQ-MSX0957 to PC) and by the Science and Technology Research Program of Chongqing Municipal Education Commission (Grant No. KJQN20230065 to HP).

Data availability

No datasets were generated or analysed during the current study.

Declarations

Consent for publication

Not applicable.

Competing interests

The authors declare no competing interests.

Received: 21 June 2024 / Accepted: 10 November 2024

Published online: 15 November 2024

References

1. Bray F, Laversanne M, Sung H, Ferlay J, Siegel RL, Soerjomataram I, et al. Global cancer statistics 2022: GLOBOCAN estimates of incidence and mortality worldwide for 36 cancers in 185 countries. *CA Cancer J Clin.* 2024;74:229–63.
2. Siegel RL, Giaquinto AN, Jemal A. Cancer statistics, 2024. *CA Cancer J Clin.* 2024;74:12–49.
3. Fan C, Oh DS, Wessels L, Weigelt B, Nuyten DS, Nobel AB, et al. Concordance among gene-expression-based predictors for breast cancer. *N Engl J Med.* 2006;355:560–9.
4. Perou CM, Sørlie T, Eisen MB, van de Rijn M, Jeffrey SS, Rees CA, et al. Molecular portraits of human breast tumours. *Nature.* 2000;406:747–52.
5. Sørlie T, Perou CM, Tibshirani R, Aas T, Geisler S, Johnsen H, et al. Gene expression patterns of breast carcinomas distinguish tumor subclasses with clinical implications. *Proc Natl Acad Sci U S A.* 2001;98:10869–74.
6. Martínez-Reyes I, Chandel NS. Cancer metabolism: looking forward. *Nat Rev Cancer.* 2021;21:669–80.
7. Snaebjornsson MT, Janaki-Raman S, Schulze A. Greasing the wheels of the cancer machine: the role of lipid metabolism in cancer. *Cell Metab.* 2020;31:62–76.
8. Luo W, Wang H, Ren L, Lu Z, Zheng Q, Ding L, et al. Adding fuel to the fire: the lipid droplet and its associated proteins in cancer progression. *Int J Biol Sci.* 2022;18:6020–34.
9. Bensaad K, Favaro E, Lewis CA, Peck B, Lord S, Collins JM, et al. Fatty acid uptake and lipid storage induced by HIF-1 α contribute to cell growth and survival after hypoxia-reoxygenation. *Cell Rep.* 2014;9:349–65.

10. Jarc E, Kump A, Malavašič P, Eichmann TO, Zimmermann R, Petan T. Lipid droplets induced by secreted phospholipase A₂ and unsaturated fatty acids protect breast cancer cells from nutrient and lipotoxic stress. *Biochim Biophys Acta Mol Cell Biol Lipids*. 2018;1863:247–65.
11. Balaban S, Lee LS, Varney B, Aishah A, Gao Q, Shearer RF, et al. Heterogeneity of fatty acid metabolism in breast cancer cells underlies differential sensitivity to palmitate-induced apoptosis. *Mol Oncol*. 2018;12:1623–38.
12. Przybytkowski E, Joly E, Nolan CJ, Hardy S, Francoeur AM, Langelier Y, et al. Upregulation of cellular triacylglycerol - free fatty acid cycling by oleate is associated with long-term serum-free survival of human breast cancer cells. *Biochem Cell Biol*. 2007;85:301–10.
13. Hershey BJ, Vazzana R, Joppi DL, Havas KM. Lipid droplets define a sub-population of breast cancer stem cells. *J Clin Med*. 2019;9:87.
14. Hultsch S, Kankainen M, Paavola L, Kovanen RM, Ikonen E, Kangaspeka S, et al. Association of tamoxifen resistance and lipid reprogramming in breast cancer. *BMC Cancer*. 2018;18(1):850.
15. Nisticò C, Pagliari F, Chiarella E, Fernandes Guerreiro J, Marafioti MG, Aversa I, et al. Lipid droplet biosynthesis impairment through DGAT2 inhibition sensitizes MCF7 breast cancer cells to radiation. *Int J Mol Sci*. 2021;22:10102.
16. Farese RV Jr, Walther TC. Glycerolipid synthesis and lipid droplet formation in the endoplasmic reticulum. *Cold Spring Harb Perspect Biol*. 2022;12:a041246.
17. Shi Y, Cheng D. Beyond triglyceride synthesis: the dynamic functional roles of MGAT and DGAT enzymes in energy metabolism. *Am J Physiol Endocrinol Metab*. 2009;297:E10–8.
18. Wang H, Airola MV, Reue K. How lipid droplets TAG along: glycerolipid synthetic enzymes and lipid storage. *Biochim Biophys Acta Mol Cell Biol Lipids*. 2017;1862:1131–45.
19. Schreiber R, Xie H, Schweiger M. Of mice and men: the physiological role of adipose triglyceride lipase (ATGL). *Biochim Biophys Acta Mol Cell Biol Lipids*. 2019;1864:880–99.
20. Zhang R, Meng J, Yang S, Liu W, Shi L, Zeng J, et al. Recent advances on the role of ATGL in cancer. *Front Oncol*. 2022;12:944025.
21. Simeone P, Tacconi S, Longo S, Lanuti P, Bravaccini S, Pirini F, et al. Expanding roles of de novo lipogenesis in breast cancer. *Int J Environ Res Public Health*. 2021;18:3575.
22. Yousuf U, Sofi S, Makhdoomi A, Mir MA. Identification and analysis of dys-regulated fatty acid metabolism genes in breast cancer subtypes. *Med Oncol*. 2022;39(12):256.
23. Shan D, Li JL, Wu L, Li D, Hurov J, Tobin JF, et al. GPAT3 and GPAT4 are regulated by insulin-stimulated phosphorylation and play distinct roles in adipogenesis. *J Lipid Res*. 2010;51:1971–81.
24. Chang P, Heier C, Qin W, Han L, Huang F, Sun Q. Molecular identification of transmembrane protein 68 as an endoplasmic reticulum-anchored and brain-specific protein. *PLoS ONE*. 2017;12:e0176980.
25. Wang Y, Zeng F, Zhao Z, He L, He X, Pang H, et al. Transmembrane protein 68 functions as an MGAT and DGAT enzyme for triacylglycerol biosynthesis. *Int J Mol Sci*. 2023;24:2012.
26. McLelland GL, Lopez-Osias M, Verzijl CRC, Ellenbroek BD, Oliveira RA, Boon NJ, et al. Identification of an alternative triglyceride biosynthesis pathway. *Nature*. 2023;621:171–8.
27. Plasterer C, Tsaih SW, Lemke A, Schilling R, Dwinell M, Rau A, et al. Identification of a rat mammary tumor risk locus that is syntenic with the commonly amplified 8q12.1 and 8q22.1 regions in human breast cancer patients. *G3 (Bethesda)*. 2019;9:1739–43.
28. Tang Z, Li C, Kang B, Gao G, Li C, Zhang Z. GEPIA: a web server for cancer and normal gene expression profiling and interactive analyses. *Nucleic Acids Res*. 2017;45:W98–102.
29. Zeng F, Heier C, Yu Q, Pang H, Huang F, Zhao Z et al. Human transmembrane protein 68 links triacylglycerol synthesis to membrane lipid homeostasis. *BioRxiv*, 2024.04.14.589399. <https://doi.org/10.1101/2024.04.14.589399>
30. Schmittgen TD, Livak KJ. Analyzing real-time PCR data by the comparative C(T) method. *Nat Protoc*. 2008;3:1101–8.
31. Heier C, Kien B, Huang F, Eichmann TO, Xie H, Zechner R, et al. The phospholipase PNPLA7 functions as a lysophosphatidylcholine hydrolase and interacts with lipid droplets through its catalytic domain. *J Biol Chem*. 2017;292:19087–98.
32. Miao H, Li B, Wang Z, Mu J, Tian Y, Jiang B et al. Lipidome atlas of the developing heart uncovers dynamic membrane lipid attributes underlying cardiac structural and metabolic maturation. *Research (Wash D C)*. 2022; 2022:0006.
33. Zhang F, Lim WLF, Huang Y, Lam SM, Wang Y. Lipidomics and metabolomics investigation into the effect of DAG dietary intervention on hyperuricemia in athletes. *J Lipid Res*. 2024;65:100605.
34. Rogers MA, Liu J, Song BL, Li BL, Chang CC, Chang TY. Acyl-CoA:cholesterol acyltransferases (ACATs/SOATs): enzymes with multiple sterols as substrates and as activators. *J Steroid Biochem Mol Biol*. 2015;151:102–7.
35. Miska J, Chandel NS. Targeting fatty acid metabolism in glioblastoma. *J Clin Invest*. 2023;133:e163448.
36. Agostini M, Melino G, Habeb B, Calandria JM, Bazan NG. Targeting lipid metabolism in cancer: neuroblastoma. *Cancer Metastasis Rev*. 2022;41:255–60.
37. Paul S, Lancaster G, Meikle PJ. Plasmalogens: a potential therapeutic target for neurodegenerative and cardiometabolic disease. *Prog Lipid Res*. 2019;74:186–95.
38. Schooneveldt YL, Paul S, Calkin AC, Meikle PJ. Ether lipids in obesity: from cells to population studies. *Front Physiol*. 2022;13:841278.
39. Lee J, Ridgway ND. Substrate channeling in the glycerol-3-phosphate pathway regulates the synthesis, storage and secretion of glycerolipids. *Biochim Biophys Acta Mol Cell Biol Lipids*. 2020;1865:158438.
40. Shindou H, Shimizu T. Acyl-CoA:lysophospholipid acyltransferases. *J Biol Chem*. 2009;284:1–5.
41. Valentine WJ, Yanagida K, Kawana H, Kono N, Noda NN, Aoki J, et al. Update and nomenclature proposal for mammalian lysophospholipid acyltransferases, which create membrane phospholipid diversity. *J Biol Chem*. 2022;298:101470.
42. Danielli M, Perne L, Jarc Jovičić E, Petan T. Lipid droplets and polyunsaturated fatty acid trafficking: balancing life and death. *Front Cell Dev Biol*. 2023;11:1104725.

Publisher's note

Springer Nature remains neutral with regard to jurisdictional claims in published maps and institutional affiliations.